International Journal of Pharmaceutics 359 (2008) 211–219

Contents lists available at ScienceDirect

International Journal of Pharmaceutics

journal homepage: www.elsevier.com/locate/ijpharm

Physicochemical properties and oral bioavailability of amorphous atorvastatin hemi-calcium using spray-drying and SAS process

Jeong-Soo Kim, Min-Soo Kim, Hee Jun Park, Shun-Ji Jin, Sibeum Lee, Sung-Joo Hwang*

National Research Laboratory of Pharmaceutical Technology, College of Pharmacy, Chungnam National University, 220 Gung-dong, Yuseong-gu, Daejeon 305-764, Republic of Korea

ARTICLE INFO

Article history:
Received 14 January 2008
Received in revised form 25 March 2008
Accepted 7 April 2008
Available online 12 April 2008

Keywords:
Atorvastatin
SAS process
Spray-drying
Amorphous
Bioavailability

ABSTRACT

The objective of the study was to prepare amorphous atorvastatin hemi-calcium using spray-drying and supercritical antisolvent (SAS) process and evaluate its physicochemical properties and oral bioavailability. Atorvastatin hemi-calcium trihydrate was transformed to anhydrous amorphous form by spray-drying and SAS process. With the SAS process, the mean particle size and the specific surface area of amorphous atorvastatin were drastically changed to 68.7 ± 15.8 nm, 120.35 ± 1.40 m^2/g and 95.7 ± 12.2 nm, 79.78 ± 0.93 m^2/g from an acetone solution and a tetrahydrofuran solution, respectively and appeared to be associated with better performance in apparent solubility, dissolution and pharmacokinetic studies, compared with unprocessed crystalline atorvastatin. Oral $AUC_{0-8\,h}$ values in SD rats for crystalline and amorphous atorvastatin were as follow: 1121.4 ± 212.0 ng h/mL for crystalline atorvastatin, 3249.5 ± 406.4 ng h/mL and 3016.1 ± 200.3 ng h/mL for amorphous atorvastatin from an acetone solution and a tetrahydrofuran solution with SAS process, 2227.8 ± 274.5 and 2099.9 ± 339.2 ng h/mL for amorphous atorvastatin from acetone and tetrahydrofuran with spray-drying. The AUCs of all amorphous atorvastatin significantly increased ($P < 0.05$) compared with crystalline atorvastatin, suggesting that the enhanced bioavailability was attributed to amorphous nature and particle size reduction. In addition, the SAS process exhibits better bioavailability than spray-drying because of particle size reduction with narrow particle size distribution. It was concluded that physicochemical properties and bioavailability of crystalline atorvastatin could be improved by physical modification such as particle size reduction and generation of amorphous state using spray-drying and SAS process. Further, SAS process was a powerful methodology for improving the physicochemical properties and bioavailability of atorvastatin.

1. Introduction

Atorvastatin, as a synthetic lipid-lowering agent, is an inhibitor of 3-hydroxy-3-methyl-glutaryl-coenzyme A (HMG-CoA) reductase which catalyzes the conversion of HMG-Co A to mevalonate, an early rate-limiting step in cholesterol biosynthesis (Lennernas, 2003). Atorvastatin is currently used as calcium salt for the treatment of hypercholesterolemia. Atorvastatin calcium ([*R*-(*R**,*R**)]-2-(4-fluorophenyl)-β,δ-dihydroxy-5-(1-methylethyl)-3-phenyl-4-[(phenylamino)carbonyl]-1H-pyrrole-1-heptanoic acid, hemi-calcium salt) is insoluble in aqueous solution of pH 4 and below; it is very slightly soluble in water and pH 7.4 phosphate buffer. The intestinal permeability of atorvastatin is high at the physiologically relevant intestinal pH (Lennernas, 1997; Wu et al., 2000). However, it is reported that the absolute bioavailability (*F*) of atorvastatin is 12% after a 40 mg oral dose (Corsini et al., 1999).

Oral bioavailability is limited by the factors such as the membrane permeability, the solubility, the dissolution rate of the drug and so on. Specially, the solubility and the dissolution rate of a poorly water-soluble drug is a critical factor for its oral bioavailability. Many approaches have been developed to improve solubility and to enhance the dissolution rate and oral bioavailability of poorly soluble drugs (e.g. salt formation (Engel et al., 2000; Perng et al., 2003; Choi et al., 2004; Han and Choi, 2007), solid dispersion (Taylor and Zografi, 1997; Chen et al., 2004; Paradkar et al., 2004; Sethia and Squillante, 2004), inclusion complex (Al-Marzouqi et al., 2006; Anzai et al., 2007; Jun et al., 2007), microemulsion (Shen and Zhong, 2006; Park et al., 2007), micronization (Farinha et al., 2000; Kim et al., 2007a), etc.). Physical modifications often aim to increase the surface area, solubility and wettability of the powder particles and are therefore focused on particle size reduction or generation of amorphous states (Hancock and Zografi, 1997; Grau et al., 2000).

* Corresponding author. Tel.: +82 42 821 5922; fax: +82 42 823 3078.
E-mail address: sjhwang@cnu.ac.kr (S.-J. Hwang).

0378-5173/$ – see front matter © 2008 Elsevier B.V. All rights reserved.
doi:10.1016/j.ijpharm.2008.04.006

An amorphous solid can be defined as its molecular arrangement lacks long-range order, which is the unique feature of crystals. Solubility (S) of a solid solute can be expressed by considering the three basic quantities, as follow (Lipinski et al., 2001);

$$S = f(\text{Crystal Packing Energy} + \text{Cavitation Energy} + \text{Solvation Energy}) \quad (1)$$

For the solubilization of a solid solute, a first major huddle to overcome is the disruption of crystal packing. A crystalline solid possess relative higher crystal packing energy, as compared to an amorphous solid. But unlike a crystalline solid, an amorphous solid has low packing energy and no long-range order of molecular packing. By this property of the amorphous solid, an amorphous solid often exhibit higher solubility than a crystalline solid. In many studies, it is reported that amorphous systems is efficient for the enhancement of dissolution and bioavailability (Mullins and Macek, 1960; Imaizumi, 1980; Sato et al., 1981; Choi et al., 2004). In addition, Hancock and Parks (2000) reported that 10–1600 folds of solubility enhancement could be achieved by the use of amorphous systems.

Recently, several studies on particle formation using the SAS process have been reported as a viable means of nanoparticle formation using various pharmaceutical compounds (Reverchon and Porta, 1999; Snavely et al., 2002; Lee et al., 2008; Marco and Reverchon, 2008). Previously, we optimized the SAS process parameters such as pressure, temperature, drug solution concentration and feeding ratio of CO_2/drug solution using methanol as a solvent (Kim et al., 2007b). Since methanol is actually a toxic solvent, we investigate the effect of solvent type on particle morphology and in vitro performances of atorvastatin particles using various ICH class III solvents such as dimethyl sulfoxide, *N*-methyl-2-pyrrolidone, acetone and tetrahydrofuran. In this study, amorphous atorvastatin was prepared by spray-drying and supercritical antisolvent (SAS) process using ICH class III solvents, acetone and tetrahydrofuran. Their physicochemical properties and oral bioavailabilities were evaluated by DSC, TGA, PXRD, solubility, dissolution and pharmacokinetic studies.

2. Materials and methods

2.1. Materials

Atorvastatin hemi-calcium trihydrate was obtained from Zhejing Jiangbei Pharmacrutic (China). Metaqualone was purchased from Sigma (St. Louis, MO, USA). Carbon dioxide (CO_2, purity 99.9%) was purchased from Hanmi Gas Co. Ltd. (Korea). Sodium laurylsulfate, extra pure grade, was purchased from Duksan Pure Chemicals (Korea). All other solvents were of HPLC grade.

2.2. Preparation of amorphous atorvastatin hemi-calcium particles

2.2.1. Supercritical anti-solvent (SAS) process

The experimental equipment used for SAS process was described in detail (Kim et al., 2007b). Briefly, CO_2 was delivered into the particle formation vessel using home-made plunger pump until equilibrium pressure and temperature (12 MPa, 40 °C) achieved. Then, drug solution (100 mg/mL in acetone or tetrahydrofuran) and supercritical CO_2 were co-injected through the two-flow spray nozzle in the particle formation vessel filled up with supercritical CO_2 at 0.5 and 45 g/min, the feed ratio (CO_2/drug solution) 90, respectively. After the injection of drug solution into the particle formation vessel, fresh CO_2 was introduced into the vessel at 45 g/min for further 120 min to remove residual solvent. During the SAS process, the pressure of the vessel controlled constantly using a back pressure regulator (Tescom®, model 26-1723-24-194). Then, the vessel was slowly depressurized and particles on the wall and the bottom of the vessel were collected.

2.2.2. Spray drying process

Atorvastatin hemi-calcium trihydrate was dissolved in acetone or tetrahydrofuran to obtain clear solutions. Spray drying was carried out using laboratory scale spray dryer (SD 1000, Eyela, Japan) under following set of conditions: drug solution concentration, 100 mg/mL; inlet temperature, 75 °C; outlet temperature, 62–65 °C; feed rate, 3 mL/min; atomization air pressure, 10 kPa; drying air flowrate, 0.70 m^3/min.

2.3. Physicochemical evaluation of amorphous particles

2.3.1. Thermal gravimetric analysis

Thermal gravimetric analysis (TGA) was carried on a TA instruments (USA) TGA 2950 Thermogravimetrical Analyzer over a temperature range of 20–300 °C at a heating rate of 5 °C/min under nitrogen flow (50 mL/min). Approximately 5 mg of sample was placed in open aluminum pans and the weight loss was monitored.

2.3.2. Differential scanning calorimetry

DSC measurements were performed using a Sinco model S-650 DSC (Korea). 2–5 mg of sample was placed in crimp sealed aluminum pans and the measurement was made over 30–200 °C at a heat rate of 5 °C/min under nitrogen flow (20 mL/min).

2.3.3. Powder X-ray diffraction

The powder X-ray diffraction patterns of samples were obtained using a Rigaku D/Max-2200 Ultima/PC powder X-ray diffraction system (Japan) with Ni-filtered Cu Kα radiation. The 2θ scan range was 5–60° with a step size of 0.02° and the scan speed was 3 °min^{-1}.

2.3.4. Particle size distribution

The particle size of unprocessed and spray-dried atorvastatin particles was determined with a HELOS laser diffraction analyzer (Sympatec Gmbh, Germany) equipped with a RODOS vibrating trough disperser. An air pressure of 0.1 MPa and a vacuum of 5.3 kPa were used to produce a uniform powder dispersion for each samples.

The size and size distribution of the SAS processed atorvastatin particles were measured by dynamic light scattering (DLS) (ELS-8000, Otsuka Electronics, Japan) with a He–Ne laser beam at a wavelength of 658 nm at room temperature and scattering angle of 90°. To obtain a complete dispersion of primary particles, the SAS processed atorvastatin particles were dispersed in mineral oil (Marcol 52, Exxon Mobil Co., USA) and then sonicated for 10 min at 120 W (Branson 8210, Branson Ul-. trasonics Co., Danbury, CT, USA).

2.3.5. BET specific surface area measurement

The specific surface area of samples was determined following the Brunauer–Emmett–Teller (BET) method of nitrogen adsorption/desorption at −196 °C with an ASAP2010 surface area analyzer (Micromeritics Instrument, USA).

2.3.6. Supersaturation in vitro analysis

A VK 7000 dissolution apparatus (VanKel, USA) using the USP XXVIII paddle method operating at a rotation speed of 200 rpm was used for supersaturation analysis of samples. All tests were carried out on excess amount (approximately 100 mg as atorvastatin) of samples. Distilled water was used as dissolution media. The volume and temperature of the dissolution medium were 200 mL and 37.0 ± 0.5 °C, respectively. Suitable aliquots

were withdrawn at predetermined time intervals and filtered using 0.11 μm nylon syringe filter. The filtrate was diluted with methanol, and the quantification of atorvastatin was performed using UV spectrophotometer at 245 nm (Mini-1240, Shimadzu, Japan). All samples were tested in triplicate.

2.3.7. Intrinsic dissolution test

The intrinsic dissolution rate (IDR) of each samples were measured using the stationary disc (Distek Inc., USA) and VK7000 dissolution apparatus (VanKel, USA) according to USP XXVIII paddle method. Intrinsic dissolution study was performed at 50 rpm and 37 ± 0.5 °C employing 900 mL of distilled water containing 1% SLS (under sink condition). To form a pellet, 80 mg of powder was compressed using a PerkinElmer hydraulic press at 5 ton force for 1 min. Analysis of the compressed pellets by DSC and FTIR confirmed that the crystal form of the original powder was retained following the compression procedure. The constant surface area of the pellet exposed was 0.5 cm^2. At predetermined time points, 3-mL aliquot samples were withdrawn with media replacement, filtered using 0.11 μm nylon syringe filter, and analyzed by a UV spectrophotometer at 245 nm. All samples were tested in triplicate.

2.3.8. Powder dissolution test

Powder dissolution tests was performed using the USP XXVIII Type II (paddle method) (VK7000, Vankel, USA). The rotation speed of the paddles was set to 50 rpm. The dissolution medium was 900 mL of deionized water. At predetermined time intervals 5 mL samples were withdrawn, filtered using 0.11 μm nylon syringe filter and the amount of dissolved drug was determined by UV spectrophotometer at 245 nm. All samples were tested in triplicate.

2.4. Pharmacokinetic study in rats

2.4.1. Animals

Male SD rats (6–7 weeks old) weighing between 180 and 200 g were purchased from Samtaco Bio Korea Inc. (Korea). All rats had free access to tap water and pelleted diet. The rats were housed in a cage and maintained on a 12 h light/dark at room temperature (25 °C) and relative humidity of 55 ± 10%. General and environmental conditions were strictly monitored. All animal experiments were performed according to the "Guidelines for the Care and Use of Laboratory Animals" at Chungnam National University. The rats were deprived of food 24 h before the experiment and food was reoffered 4 h post-dosing. The rats were divided into five groups of five animals each. Each group was administered orally 1 mL of 0.2% (w/v) methylcellulose aqueous suspensions containing unprocessed atorvastatin, SAS processed atorvastatin particles precipitated from an acetone solution (SCFA), SAS processed atorvastatin particles precipitated from a tetrahydrofuran solution (SCFT), spray-dried atorvastatin particles from an acetone solution (SDA) and spray-dried atorvastatin particles from a tetrahydrofuran solution (SDT) (equivalent to 25 mg/kg body weight as atorvastatin), respectively. Blood samples were collected by tail vein; predose, 15, 30, 45, 60, 90, 120, 240, 360 and 480 min post-dosing. Blood samples were held on ice (+4 °C) until centrifuged at 10,000 rpm, 4 °C for 10 min. Plasma was transferred to individual Eppendorf's and stored at −20 °C until analyzed.

2.4.2. LC/MS instrument and conditions

The LC/MS system consisted of a LC-10ADvp pump, SIL-10A autoinjector, SPD-10ADvp UV detector, and LCMS-2010A mass spectrometer (Shimadzu, Japan). The analytical column was Kromasil C_{18} (150 mm × 4.6 mm, 5 μm) and the detection wavelength was 270 nm. The mobile phase consisted of 0.1 M ammonium acetate buffer (pH 4.0)/acetonitrile (50:50, v/v) was pumped at a flow rate of 1 mL/min.

The mass spectrometer was operated in positive ion mode and connected to the system using an API electrospray interface. The $[M+H]^+$, m/z 251.00 for methaqualone and $[M+H]^+$, m/z 559.00 for atorvastatin were selected as detecting ions, respectively (Hermann et al., 2005; Nirogi et al., 2006). The MS operating conditions were optimized as follows: drying gas 1.5 L/min, CDL temperature 250 °C, block temperature 200 °C and probe voltage: +4.5 kV. Data processing was performed using the LCMS solution software (Shimadzu, Japan).

2.4.3. Plasma sample preparation

A plasma sample (200 μL) was spiked with 100 μL of internal standard solution (methaqualone, 100 ng/mL) and 700 μL of acetonitrile was added. After vortex mixing for 30 s, 800 μL of supernatant was carefully transferred to a 15 mL glass test tube and evaporated to dryness using a centrifugal evaporator (CVE-2000, Eyela, Japan). Then the dried residual was reconstituted in 200 μL of methalol and a 5 μL aliquot was injected into the LC/MS system for the quantification of atorvastatin.

2.4.4. Statistical analysis

Model independent pharmacokinetic parameters were calculated using WinNonLin Version 2.1 (Pharsight Corp., Mountain View, CA). The PK data between different formulations were compared for statistical significance ($P < 0.05$) by the one-way ANOVA followed by Tukey–HSD multiple comparisons test using SPSS v 12.0 software (SPSS, Chicago, IL, USA).

3. Results and discussion

3.1. Physicochemical evaluation of amorphous particles

In this study, amorphous atorvastatin particles were obtained from two organic solvents, acetone and tetrahydrofuran, containing atorvastatin hemi-calcium trihydrate. DSC, TGA and PXRD analysis and pharmaceutically important solid-state properties including solubility, dissolution, and intrinsic dissolution were studied to characterize the particles obtained by SAS process and spray-drying process.

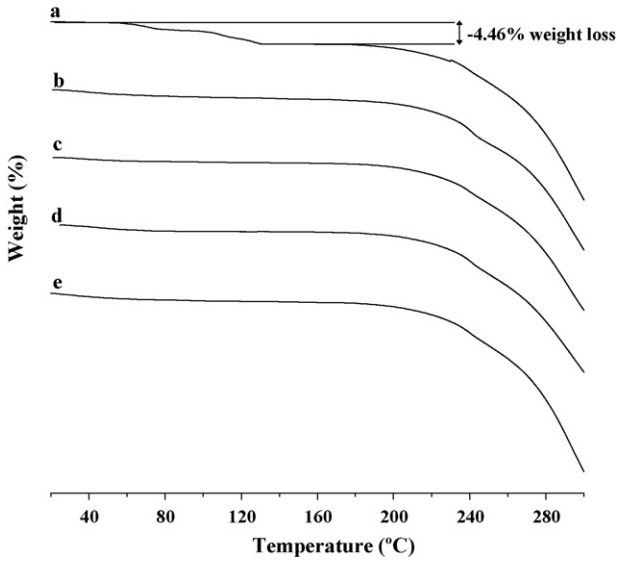

Fig. 1. TGA curves of (a) unprocessed atorvastatin particles, crystalline, (b) SAS processed amorphous atorvastatin calcium precipitated from an acetone solution, (c) SAS processed amorphous atorvastatin calcium precipitated from a tetrahydrofuran solution, (d) spray-dried amorphous atorvastatin calcium from an acetone solution and (e) spray-dried amorphous atorvastatin calcium from a tetrahydrofuran solution.

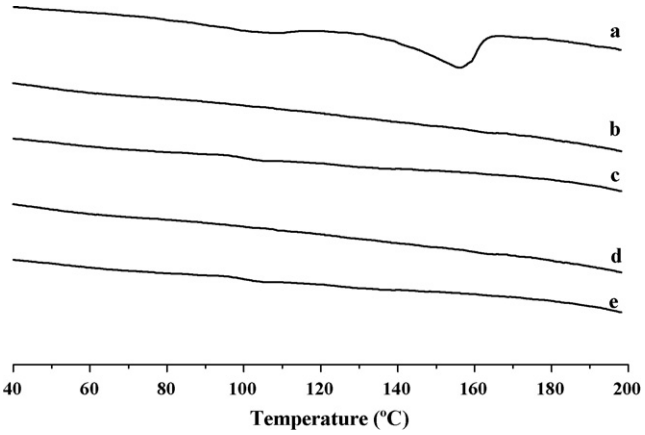

Fig. 2. DSC traces of (a) unprocessed atorvastatin particles, crystalline, (b) SAS processed amorphous atorvastatin calcium precipitated from an acetone solution, (c) SAS processed amorphous atorvastatin calcium precipitated from a tetrahydrofuran solution, (d) spray-dried amorphous atorvastatin calcium from an acetone solution and (e) spray-dried amorphous atorvastatin calcium from a tetrahydrofuran solution.

The TGA curves of unprocessed, SAS processed and spray-dried atorvastatin particles are shown in Fig. 1. Theoretically the stoichiometric value of the trihydrate should be 4.46%. Unprocessed particles exhibited a gradual decrease in weight about 4.46% due to the loss of water. The total weight loss corresponding to a water loss of about 4.46% is in agreement with stoichiometric value of a trihydrate. On the other hand, this weight loss was not seen for all processed particles. From these TGA results, it can be seen that unprocessed atorvastatin, atorvastatin calcium trihydrate, were transformed to anhydrous from by both of SAS and spray drying process (Kim et al., 2007b).

Fig. 2 shows the DSC curves of unprocessed and all processed particles. The DSC curves of unprocessed atorvastatin, a broad endotherm at 50–130 °C and a sharp endotherm at 155.96 °C were observed. The broad endotherm ranging from 50 to 130 °C indicating the loss of water was consistent with the result of TGA. The sharp endotherm at 155.96 °C might be due to the melting point of atorvastatin calcium. However, no endotherms were observed in the DSC curves for SCFA, SCFT, SDA and SDT. The powder X-ray diffraction patterns of unprocessed and processed particles are shown in Fig. 3. Characteristic diffraction peaks at $2\theta = 9.12$, 9.44, 10.23, 10.54, 11.82, 12.16, 16.97, 19.45, 21.59, 22.62, 23.22 and 23.68° were observed for unprocessed atorvastatin. On the other hand, all processed particles were characterized by the complete absence of any diffraction peak corresponding to crystalline atorvastatin calcium. These results indicate that atorvastatin is no longer present as a crystalline form when processed using SAS and spray-drying, but exists in the amorphous state.

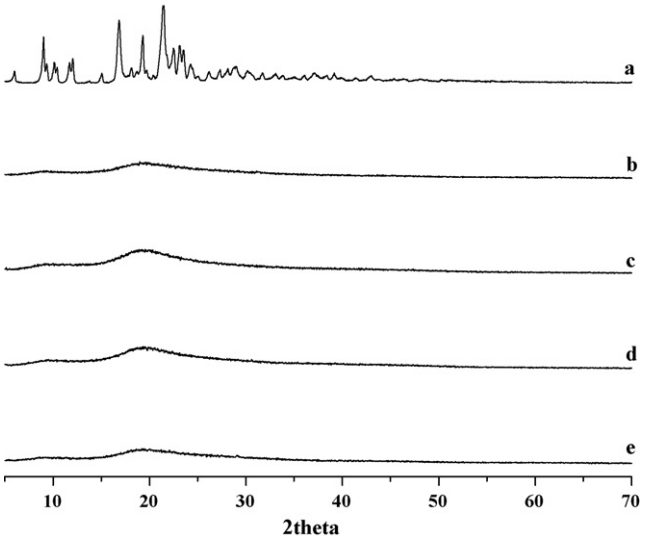

Fig. 3. XRD patterns for unprocessed atorvastatin particles (■), SAS processed amorphous atorvastatin calcium precipitated from an acetone solution (●), SAS processed amorphous atorvastatin calcium precipitated from a tetrahydrofuran solution (▲), spray-dried amorphous atorvastatin calcium from an acetone solution (○) and spray-dried amorphous atorvastatin calcium from a tetrahydrofuran solution(□).

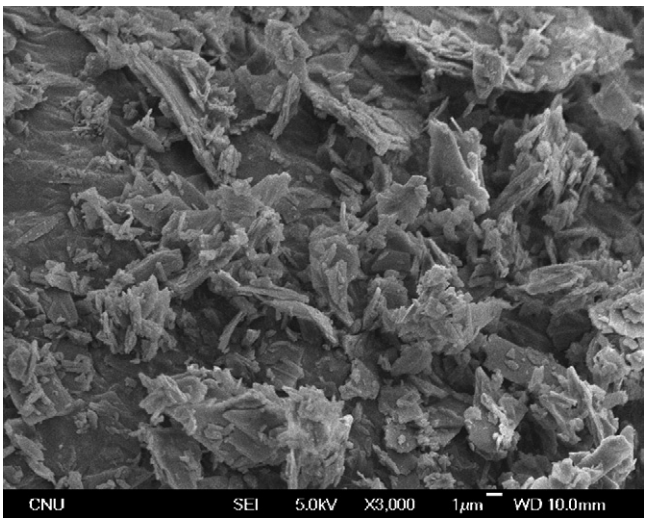

Fig. 4. SEM micrograph of unprocessed atorvastatin particles, crystalline (×3000).

The SEM images of unprocessed and processed atorvastatin particles are presented in Figs. 4–8. While unprocessed atorvastatin particles have appeared as irregular-shaped crystals, a drastic change in the morphology and shape of drug was observed for all processed particles. SAS processed particles, SCFA and SCFT, were observed as spherical agglomerated nanoparticles. The particle size and specific surface area of unprocessed and all processed particles are summarized in Table 1. The SAS processed particles exhibit narrow size distribution with a mean particle size of 68.7 ± 15.8 and 95.7 ± 12.2 nm for SCFA and SCFT, respectively (Fig. 9). On the

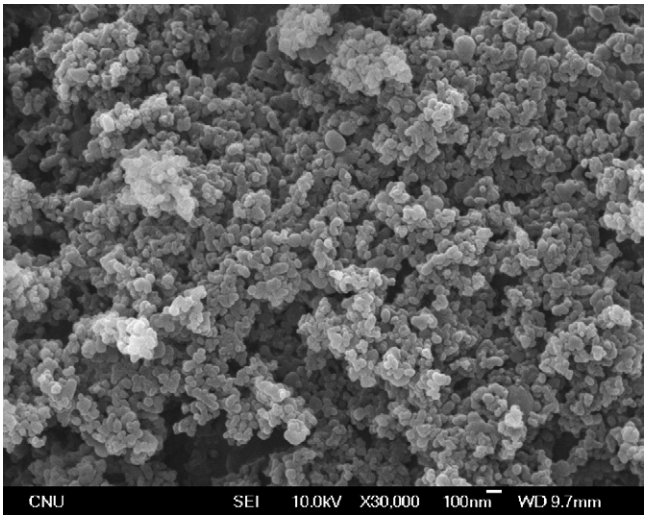

Fig. 5. SEM micrograph of SAS processed amorphous atorvastatin calcium precipitated from an acetone solution (×30,000).

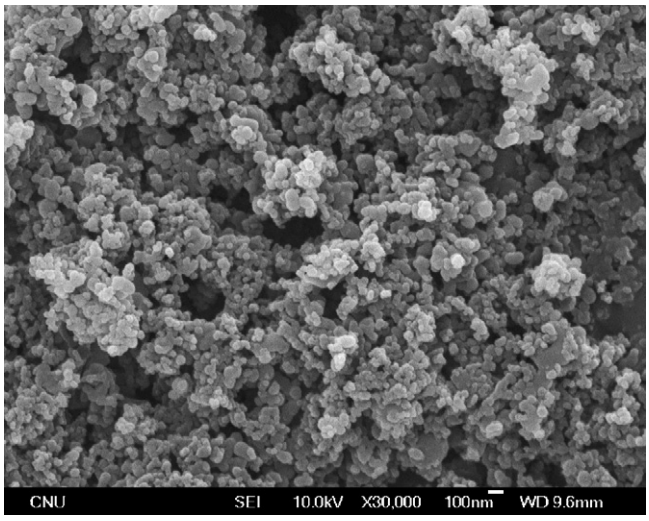

Fig. 6. SEM micrograph of SAS processed amorphous atorvastatin calcium precipitated from a tetrahydrofuran solution (×30,000).

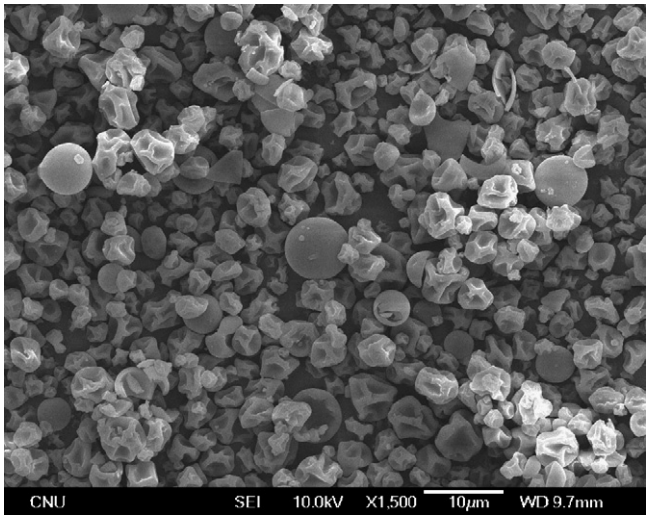

Fig. 7. SEM micrograph of spray-dried amorphous atorvastatin calcium from an acetone solution (×1500).

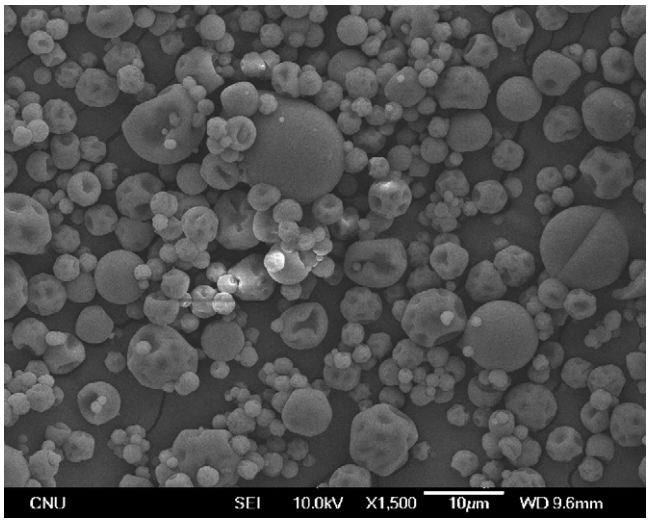

Fig. 8. SEM micrograph of spray-dried amorphous atorvastatin calcium from a tetrahydrofuran solution (×1500).

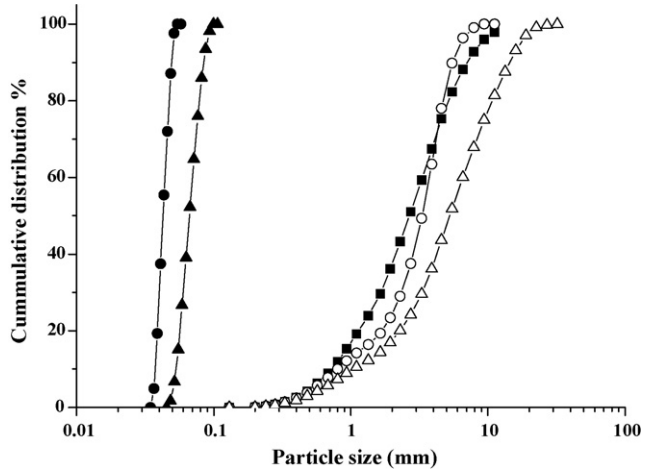

Fig. 9. Cumulative particle size distributions curves for unprocessed atorvastatin particles (■), SAS processed amorphous atorvastatin calcium precipitated from an acetone solution (●), SAS processed amorphous atorvastatin calcium precipitated from a tetrahydrofuran solution (▲), spray-dried amorphous atorvastatin calcium from an acetone solution (○) and spray-dried amorphous atorvastatin calcium from a tetrahydrofuran solution(□).

other hand, the spray-dried particles were observed as irregular shaped microparticles with a mean particle size of 3.62 ± 0.15 and 7.31 ± 0.21 μm for SDA and SDT, respectively. Specially, the specific surface area of the SAS processed particles were increased significantly, 120.35 ± 1.40 and 79.78 ± 0.93 m^2/g for SCFA and SCFT, respectively, compared with unprocessed atorvastatin. In the case of SAS processed particles, the increased surface area might be due to the particle size reduction achieved by the SAS process.

The supersaturated dissolution patterns of unprocessed and processed atorvastatin particles are shown in Fig. 10. In the case of unprocessed atorvastatin particles, the equilibrium solubility (approximately 140 μg/mL) was reached rapidly. In contrast, the maximum supersaturated concentrations of atorvastatin from all processed particles were almost similar and were about 460 μg/mL. However, the supersaturated concentration of atorvastatin decreased gradually to about 200 μg/mL after 24 h. It is suggested that these dissolution behaviors of all processed particles might be due to the amorphous nature. In other words, the lack of long-range molecular order and higher Gibbs free energy of amor-

Table 1
Mean particle sizes of crystalline atorvastatin calcium and amorphous atorvastatin calcium (mean ± S.D.; $n = 3$)

	Unprocessed atorvastatin	SAS processed		Spray-dried	
		From acetone (SCFA)	From tetrahydrofuran (SCFT)	From acetone (SDA)	From tetrahydrofuran (SDT)
Mean particle size	3.83 ± 0.08 μm [a]	68.7 ± 15.8 nm [b]	95.7 ± 12.2 nm [b]	3.62 ± 0.15 μm [a]	7.31 ± 0.21 μm [a]
BET surface area (m^2/g)	14.56 ± 0.17	120.35 ± 1.40	79.78 ± 0.93	3.69 ± 0.06	0.95 ± 0.03

[a] Measured value using HELOS laser diffraction analyzer.
[b] Measured value using ELS-8000 electrophoretic light scattering spectrophotometer.

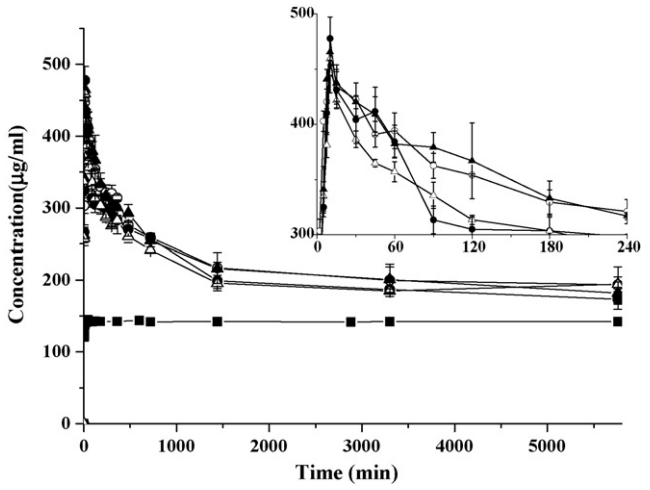

Fig. 10. Kinetics to saturation solubility for unprocessed atorvastatin particles (■), SAS processed amorphous atorvastatin calcium precipitated from an acetone solution (●), SAS processed amorphous atorvastatin calcium precipitated from a tetrahydrofuran solution (▲), spray-dried amorphous atorvastatin calcium from an acetone solution (○) and spray-dried amorphous atorvastatin calcium from a tetrahydrofuran solution (□) ($n = 3$, mean ± S.D.).

phous form resulted in rapid dissolution, reflected as the maximum supersaturated concentration value after 10 min (Elamin et al., 1994; Chawla and Bansal, 2007). Then, the maximum supersaturated concentration of amorphous particles was decreased due to solvent-mediated conversion from the amorphous to crystalline form. Nevertheless, the increased concentration of atorvastatin, above 300 μg/mL, was maintained during 3 h.

Intrinsic dissolution patterns of unprocessed and processed atorvastatin particles, SAS processed particles and spray-dried particles are shown in Fig. 11. Good linearities between time and released amount per unit area were found for unprocessed atorvastatin particles. However, a decrease in the slope can be observed after 10 min for all processed particles. This phenomenon might be also due to solvent-mediated conversion from the amorphous to crystalline form.

Under sink conditions, the intrinsic dissolution rate J of a solid is given by:

$$J = kC_s \tag{2}$$

where k is the intrinsic dissolution rate constant given by the ratio of the solid diffusivity and the thickness of the diffusion layer. Since hydrodynamic conditions are identical, the intrinsic dissolution rate constant of unprocessed atorvastatin and all processed particles must be equal. Then Eq. (2) yields:

$$J_{\text{crystalline}}/J_{\text{amorphous}} = C_{\text{crystalline}}/C_{\text{amorphous}} \tag{3}$$

where $J_{\text{crystalline}}$ and $J_{\text{amorphous}}$ are the intrinsic dissolution rate for unprocessed atrovastatin (crystalline form) and processed atrovastatin (amorphous form), and $C_{\text{crystalline}}$ and $C_{\text{amorphous}}$ are the solubilities of unprocessed and processed atrovastatin, respectively. Therefore, knowing the values for $J_{\text{crystalline}}$, $J_{\text{amorphous}}$ and $C_{\text{crystalline}}$, the value for $C_{\text{amorphous}}$ can be readily calculated (Khankari and Grant, 1995; Di Martino et al., 2001). The intrinsic dissolution rates, the observed supersaturated concentrations, the observed solubilities for atorvastatin particles and the estimated solubilities for amorphous atorvastatin are listed in Table 2. Intrinsic dissolution rate of unprocessed atorvastatin was only 84.9 μg/min/cm^2. On the other hand, in comparison to spray-dried particles (280.1 and 278.9 μg/min/cm^2 for SDA and SDT, respectively), SAS processed atorvastatin particles exhibited similar intrinsic dissolution rates 288.5 and 280.7 μg/min/cm^2 for SCFA and SCFT, respectively. The intrinsic dissolution rate of amorphous atorvastatin particles were increased 3.5 folds compared with the intrinsic dissolution rate of crystalline atorvastatin. In addition, the estimated solubilities for amorphous samples, calculated by Eq. (3), were in good agreement with the maximum supersaturated concentrations observed from supersaturated dissolution test. Generally, compounds with intrinsic dissolution rate below 0.1 mg/min/cm^2 exhibited problems with dissolution rate-limited absorption (Kaplan, 1972). Since the intrinsic dissolution rate of crystalline atorvastatin was 0.0849 mg/min/cm^2, atorvastatin is a drug with dissolution rate-limited absorption. Thus, the higher intrinsic dissolution rate values for amorphous atorvastatin particles means that amorphous system can provide a way to improve the bioavailability of atorvastatin.

Powder dissolution profiles for unprocessed and processed particles are shown in Fig. 12. Dissolution rate enhancement is clearly observed for SAS processed and spray-dried particles with comparison of unprocessed atorvastatin. Approximately 90% and 65% of the atorvastatin was already dissolved after 10 min for SAS processed particles and spray-dried particles, respectively, compared to dissolution of below 50% of unprocessed atorvastatin after the same time period. Complete drug dissolution being reached after only 15 min for SAS processed particles. Specially, SAS processed particles exhibited faster dissolution than spray-dried particles. This can be explained by reduced particles size of SAS processed particles. The SAS process decreased the size of solid particles to the nanometer scale and simultaneously increased the surface area of particles dramatically. By the increase in surface area, the high energy state which achieved will increase the extent to which the particles can dissolve due to an increase in dissolution pressure in regards to Noyes–Whitney and Ostwald–Freundlich equations (Brittain, 1995; Vaughn et al., 2006). Therefore, these results in faster dissolution rate of the SAS processed particles, compared with that of spray-dried particles.

3.2. Pharmacokinetic study

Following an oral dose of 25 mg/kg (as atorvastatin), pharmacokinetic study was carried out on male SD rats and pharmacokinetic parameters were calculated. Fig. 13 shows the pharmacokinetic profiles for each sample and pharmacokinetic parameters are summarized in Table 3. The amorphous atorvastatin particles from SAS process and spray-drying exhibited significantly increased $AUC_{0-8\,h}$ and C_{max} compared with unprocessed atorvastatin (crystalline). Absorption of a drug is considered to involve a dissolution step of the drug into the luminal fluid followed by transport across the gastrointestinal epithelium. The low solubility and/or the dissolution rate may become the rate-determining step in the bioavailability pathway. The crystalline atorvastatin has, due to the lattice energy gain, a lower free energy and, hence, a lower solubility and than the amorphous atorvastatin. Therefore, the amorphous atorvastatin permitted to obtain high degree of supersaturation by contrast with the crystalline atorvastatin. It is suggested that the amorphous atorvastatin allows higher apparent solubilities, thereby increasing the concentration of drug available for absorption.

The AUC of unprocessed and processed atorvastatin particles were in order of SCFA > SCFT > SDA > SDT > unprocessed atorvastatin particles. The C_{max} of unprocessed and processed atorvastatin particles were in order of SCFA > SCFT > SDT > SDA > unprocessed atorvastatin particles. The differences in bioavailability between SAS processed particles and spray-dried particles should be attributed to the differences in surface area of particles. The mean

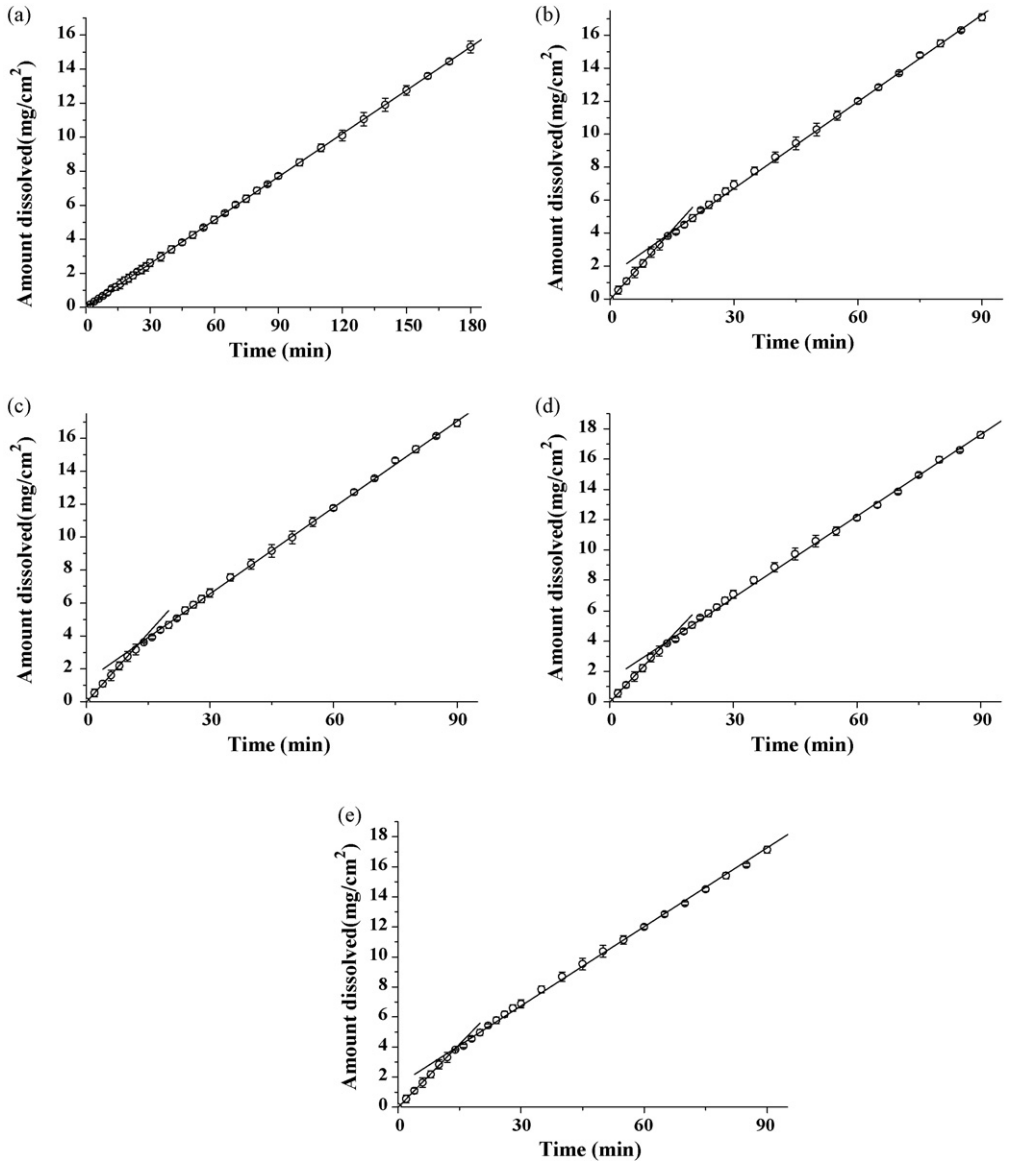

Fig. 11. Intrinsic dissolution patterns of (a) unprocessed atorvastatin particles, crystalline, (b) SAS processed amorphous atorvastatin calcium precipitated from an acetone solution, (c) SAS processed amorphous atorvastatin calcium precipitated from a tetrahydrofuran solution, (d) spray-dried amorphous atorvastatin calcium from an acetone solution and (e) spray-dried amorphous atorvastatin calcium from a tetrahydrofuran solution ($n = 3$, mean ± S.D.).

Table 2
Intrinsic dissolution rates and solubilities of crystalline atorvastatin calcium and amorphous atorvastatin calcium in water at 37 °C

	Intrinsic dissolution rate (μg/min/cm^2)		Solubility (μg/mL)	
Unprocessed atorvastatin (crystalline form)	84.9		142.2[a]	
	Early-phase (until 10 min)	Late-phase	Estimated solubility	Peak concentration[c]
SAS processed (amorphous form)				
From acetone (SCFA)	288.5	179.5	483.2[b]	477.8[c]
From tetrahydrofuran (SCFT)	280.7	175.4	470.1[b]	465.4[c]
Spray-dried (amorphous form)				
From acetone (SDA)	280.1	175.6	469.1[b]	447.2[c]
From tetrahydrofuran (SDT)	278.9	175.1	467.1[b]	459.2[c]

[a] Observed value.
[b] Calculated value using Eq. (2).
[c] Observed maximum supersaturated concentration.

Table 3
Pharmacokinetic parameters of crystalline atorvastatin calcium and amorphous atorvastatin calcium after oral administration in SD rats (mean ± S.D.; $n = 5$)

	$AUC_{0-8\,h}$ (ng h/mL)	C_{max} (ng/mL)	T_{max} (h)
Unprocessed atorvastatin (crystalline form)	1121.4 ± 212.0	504.4 ± 66.4	0.6 ± 0.1
SAS processed (amorphous form)			
From acetone (SCFA)	3249.5 ± 406.4[a,b,c]	2133.4 ± 353.2[a,b,c,d]	0.3 ± 0.0
From tetrahydrofuran (SCFT)	3016.1 ± 200.3[a,b,c]	1636.9 ± 137.9[a,b,c]	0.3 ± 0.0
Spray-dried (amorphous form)			
From acetone (SDA)	2227.8 ± 274.5[a]	939.3 ± 170.8[a]	0.3 ± 0.0
From tetrahydrofuran (SDT)	2099.9 ± 339.2[a]	1050.0 ± 136.8[a]	0.3 ± 0.0

[a] Indicating significant ($P < 0.05$) compared to unprocessed atorvastatin (crystalline).
[b] Indicating significant ($P < 0.05$) compared to spray-dried amorphous atorvastatin from an acetone solution.
[c] Indicating significant ($P < 0.05$) compared to spray-dried amorphous atorvastatin from a tetrahydrofuran solution.
[d] Indicating significant ($P < 0.05$) compared to SAS processed amorphous atorvastatin from a tetrahydrofuran solution.

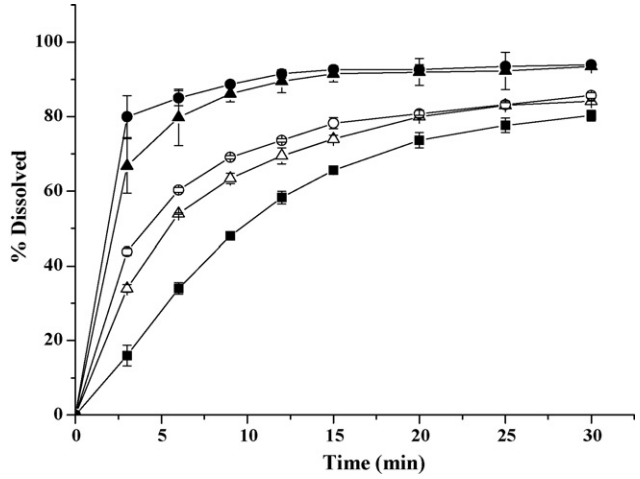

Fig. 12. Powder dissolution profiles of unprocessed atorvastatin particles (■), SAS processed amorphous atorvastatin calcium precipitated from an acetone solution (●), SAS processed amorphous atorvastatin calcium precipitated from a tetrahydrofuran solution (▲), spray-dried amorphous atorvastatin calcium from an acetone solution (○) and spray-dried amorphous atorvastatin calcium from a tetrahydrofuran solution (□) ($n = 3$, mean ± S.D.).

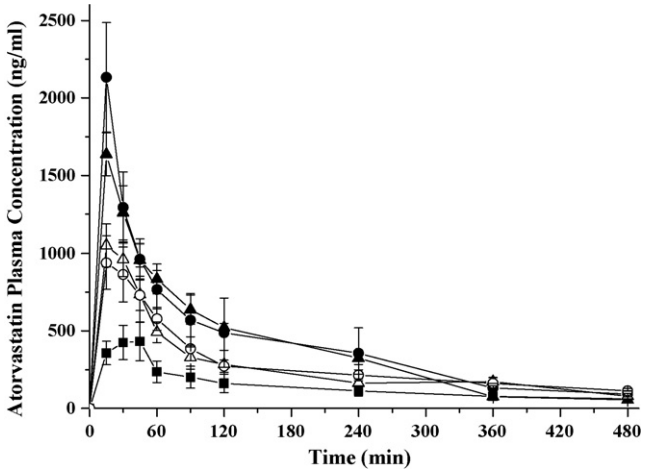

Fig. 13. Plasma concentration–time curves of unprocessed atorvastatin particles (■), SAS processed amorphous atorvastatin calcium precipitated from an acetone solution (●), SAS processed amorphous atorvastatin calcium precipitated from a tetrahydrofuran solution (▲), spray-dried amorphous atorvastatin calcium from an acetone solution (○) and spray-dried amorphous atorvastatin calcium from a tetrahydrofuran solution (□) ($n = 5$, mean ± S.D.).

particle size of spray-dried particles was 40–100 folds larger compared with that of SAS processed particles. As seen in Fig. 7, since the SAS process decreased the particle size to low nanometer range and thereby increased the surface area dramatically, the dissolution rate of SAS processed particles was faster than those of spray-dried particles. Thus, it is suggested that SAS processed particles could exhibit enhanced bioavailability compared with spray-dried particles.

4. Conclusions

In this study, amorphous atorvastatin calcium was successfully prepared by spray-drying and SAS process and evaluated its physicochemical properties and bioavailability. Through the physicochemical assessment, amorphous atorvastatin was anhydrous form and exhibit enhanced dissolution rate and higher apparent solubility due to their amorphous nature, compared with crystalline atorvastatin. Also, it exhibits dramatic enhancement in oral bioavailability. The enhancement in oral bioavailability of amorphous atorvastatin was attributed to a combination of higher apparent solubility and higher dissolution rate due to amorphous nature. This study demonstrated the usefulness of the amorphous system as a method of enhancing the dissolution of atorvastatin. Furthermore, the SAS process is an efficient tool for improving oral bioavailability of atorvastatin in combination of the benefit of amorphous form and surface area maximization.

Acknowledgments

This work was supported by the Korea Science and Engineering Foundation (KOSEF) through the National Research Lab. Program funded by the Ministry of Science and Technology (No. M10300000301-06J0000-30110) and by the Energy Conservation Technology Program (2004-E-ID12-P-05-3-010).

References

Al-Marzouqi, A., Shehatta, I., Jobe, B., Dowaidar, A., 2006. Phase solubility and inclusion complex of itraconazole with beta-cyclodextrin. J. Pharm. Sci. 95, 292–304.
Anzai, K., Mizoguchi, J., Yanagi, T., Hirayama, F., Arima, H., Uekama, K., 2007. Improvement of dissolution properties of a new Helicobacter pylori eradicating agent (TG44) by inclusion complexation with beta-cyclodextrin. Chem. Pharm. Bull. (Tokyo) 55, 1466–1470.
Brittain, H., 1995. Physical Characterization of Pharmaceutical Solids. Marcel Dekker, New York.
Chawla, G., Bansal, A., 2007. A comparative assessment of solubility advantage from glassy and crystalline forms of a water-insoluble drug. Eur. J. Pharm. Sci. 32, 45–57.
Chen, Y., Zhang, G., Neilly, J., Marsh, K., Mawhinney, D., Sanzgiri, Y., 2004. Enhancing the bioavailability of ABT-963 using solid dispersion containing Pluronic F-68. Int. J. Pharm. 286, 69–80.

Choi, W.S., Kim, H.I., Kwak, S.S., Chung, H.Y., Chung, H.Y., Yamamoto, K., Oguchi, T., Tozuka, Y., Yonemochi, E., Terada, K., 2004. Amorphous ultrafine particle preparation for improvement of bioavailability of insoluble drugs: grinding characteristics of fine grinding mills. Int. J. Miner. Process. 74, S165–S172.

Corsini, A., Bellosta, S., Baetta, R., Fumagalli, R., Paoletti, R., Bernini, F., 1999. New insights into the pharmacodynamic and pharmacokinetic properties of statins. Pharmacol. Ther. 84, 413–428.

Di Martino, P., Barthelemy, C., Palmieri, G., Martelli, S., 2001. Physical characterization of naproxen sodium hydrate and anhydrate forms. Eur. J. Pharm. Sci. 14,293–300.

Elamin, A.A., Ahlneck, C., Alderborn, G., Nystrom, C., 1994. Increased metastable solubility of milled griseofulvin, depending on the formation of a disordered surface structure. Int. J. Pharm. 111, 159–170.

Engel, G., Farid, N., Faul, M., Richardson, L., Winneroski, L., 2000. Salt form selection and characterization of LY333531 mesylate monohydrate. Int. J. Pharm. 198, 239–247.

Farinha, A., Bica, A., Tavares, P., 2000. Improved bioavailability of a micronized megestrol acetate tablet formulation in humans. Drug Dev. Ind. Pharm. 26,567–570.

Grau, M.J., Kayser, O., Muller, R.H., 2000. Nanosuspensions of poorly soluble drugs—reproducibility of small scale production. Int. J. Pharm. 196, 155–159.

Han, H.-K., Choi, H.-K., 2007. Improved absorption of meloxicam via salt formation with ethanolamines. Eur. J. Pharm. Biopharm. 65, 99–103.

Hancock, B., Parks, M., 2000. What is the true solubility advantage for amorphous pharmaceuticals? Pharm. Res. 17, 397–404.

Hancock, B.C., Zografi, G., 1997. Characteristics and significance of the amorphous state in pharmaceutical systems. J. Pharm. Sci. 86, 1–12.

Hermann, M., Christensen, H., Reubsaet, J., 2005. Determination of atorvastatin and metabolites in human plasma with solid-phase extraction followed by LC-tandem MS. Anal. Bioanal. Chem. 382, 1242–1249.

Imaizumi, H., 1980. Stability and several physical properties of amorphous and crystalline forms of indomethacin. Chem. Pharm. Bull. (Tokyo) 29, 983–987.

Jun, S., Kim, M., Kim, J., Park, H., Lee, S., Woo, J., Hwang, S., 2007. Preparation and characterization of simvastatin/hydroxypropyl-beta-cyclodextrin inclusion complex using supercritical antisolvent (SAS) process. Eur. J. Pharm. Biopharm. 66, 413–421.

Kaplan, S.A., 1972. Biopharmaceutical considerations in drug formulation design and evaluation. Drug Metab. Rev. 1, 15–34.

Khankari, R.K., Grant, D.J.W., 1995. Pharmaceutical hydrates. Thermochim. Acta 248, 61–79.

Kim, M.-S., Lee, S., Park, J.-S., Woo, J.-S., Hwang, S.-J., 2007a. Micronization of cilostazol using supercritical antisolvent (SAS) process: effect of process parameters. Powder Technol. 177, 64–70.

Kim, M.-S., Jin, S.-J., Kim, J.-S., Park, H.J., Song, H.-S., Neubertb, R.H.H., Hwang, S.-J., 2007b. Preparation, characterization and in vivo evaluation of amorphous atorvastatin calcium nanoparticles using supercritical antisolvent (SAS) process. Eur. J. Pharm. Biopharm..

Lee, L.Y., Wang, C.H., Smith, K.A., 2008. Supercritical antisolvent production of biodegradable micro- and nanoparticles for controlled delivery of paclitaxel. J. Control. Release 125, 96–106.

Lennernas, H., 1997. Human jejunal effective permeability and its correlation with preclinical drug absorption models. J. Pharm. Pharmacol. 49, 627–638.

Lennernas, H., 2003. Clinical pharmacokinetics of atorvastatin. Clin. Pharmacokinet. 42, 1141–1160.

Lipinski, C., Lombardo, F., Dominy, B., Feeney, P., 2001. Experimental and computational approaches to estimate solubility and permeability in drug discovery and development settings. Adv. Drug Deliv. Rev. 46, 3–26.

Marco, I.D., Reverchon, E., 2008. Supercritical antisolvent micronization of cyclodextrins. Powder Technol. 183, 239–246.

Mullins, J., Macek, T., 1960. Some pharmaceutical properties of novobiocin. J. Am. Pharm. Assoc. 49, 245–248.

Nirogi, R., Kandikere, V., Shukla, M., Mudigonda, K., Maurya, S., Boosi, R., Anjaneyulu, Y., 2006. Simultaneous quantification of atorvastatin and active metabolites in human plasma by liquid chromatography-tandem mass spectrometry using rosuvastatin as internal standard. Biomed. Chromatogr. 20, 924–936.

Paradkar, A., Ambike, A., Jadhav, B., Mahadik, K., 2004. Characterization of curcumin-PVP solid dispersion obtained by spray drying. Int. J. Pharm. 271, 281–286.

Park, M., Ren, S., Lee, B., 2007. In vitro and in vivo comparative study of itraconazole bioavailability when formulated in highly soluble self-emulsifying system and in solid dispersion. Biopharm. Drug Dispos. 28, 199–207.

Perng, C., Kearney, A., Palepu, N., Smith, B., Azzarano, L., 2003. Assessment of oral bioavailability enhancing approaches for SB-247083 using flow-through cell dissolution testing as one of the screens. Int. J. Pharm. 250, 147–156.

Reverchon, E., Porta, G.D., 1999. Production of antibiotic micro- and nano-particles by supercritical antisolvent precipitation. Powder Technol. 106, 23–29.

Sato, T., Okada, A., Sekiguchi, K., Tsuda, Y., 1981. Difference in physico-pharmaceutical properties between crystalline and non-crystalline 9,3″-diacetylmidecamycin. Chem. Pharm. Bull. (Tokyo) 29, 2675–2682.

Sethia, S., Squillante, E., 2004. Solid dispersion of carbamazepine in PVP K30 by conventional solvent evaporation and supercritical methods. Int. J. Pharm. 272, 1–10.

Shen, H., Zhong, M., 2006. Preparation and evaluation of self-microemulsifying drug delivery systems (SMEDDS) containing atorvastatin. J. Pharm. Pharmacol. 58, 1183–1191.

Snavely, W.K., Subramaniam, B., Rajewski, R.A., Defelippis, M.R., 2002. Micronization of insulin from halogenated alcohol solution using supercritical carbon dioxide as an antisolvent. J. Pharm. Sci. 91, 2026–2039.

Taylor, L., Zografi, G., 1997. Spectroscopic characterization of interactions between PVP and indomethacin in amorphous molecular dispersions. Pharm. Res. 14, 1691–1698.

Vaughn, J., McConville, J., Crisp, M., Johnston, K., Williams III., R., 2006. Supersaturation produces high bioavailability of amorphous danazol particles formed by evaporative precipitation into aqueous solution and spray freezing into liquid technologies. Drug Dev. Ind. Pharm. 32, 559–567.

Wu, X., Whitfield, L.R., Stewart, B.H., 2000. Atorvastatin transport in the Caco-2 Cell Model: contributions of P-glycoprotein and the proton-monocarboxylic acid co-transporter. Pharm. Res. 17, 209–215.